Supporting Information

Ultralight and Mechanically Robust Carbon Monolith with Aligned Microchannels

Minghao Liu, Masataka Inoue, Hirotaka Nakatsuji, Rui Tang, Zheng-Ze Pan, Hirotomo Nishihara**

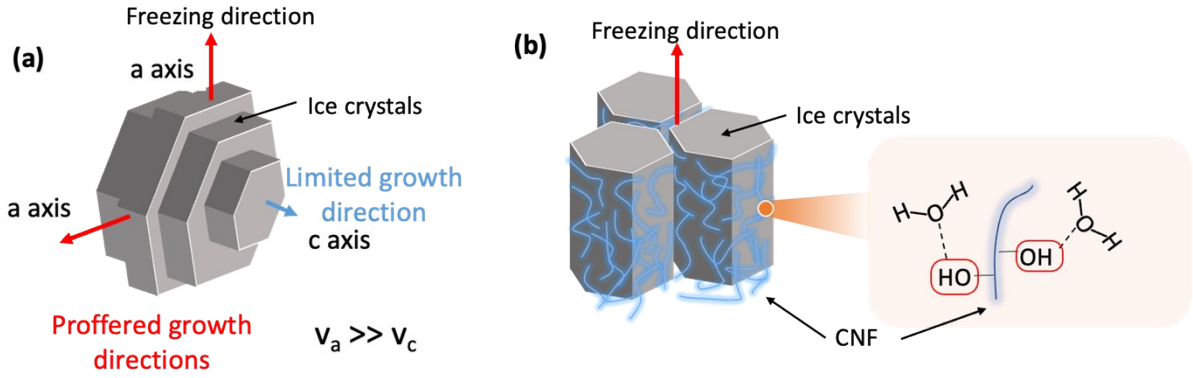

Figure S1. Illustrations of ice crystal growth. (a) lamellar growth without CNFs. (b) honeycomb-directed growth with CNFs.

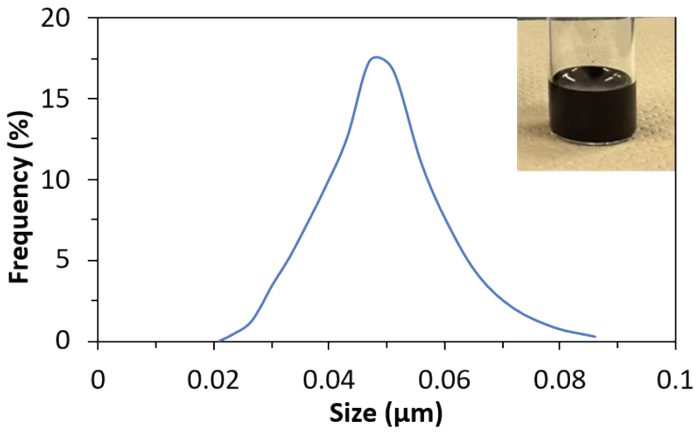

Figure S2. Particle-size distribution of carbon black (CB) used in this work. The inset image is an optical image of CB dispersed in water.

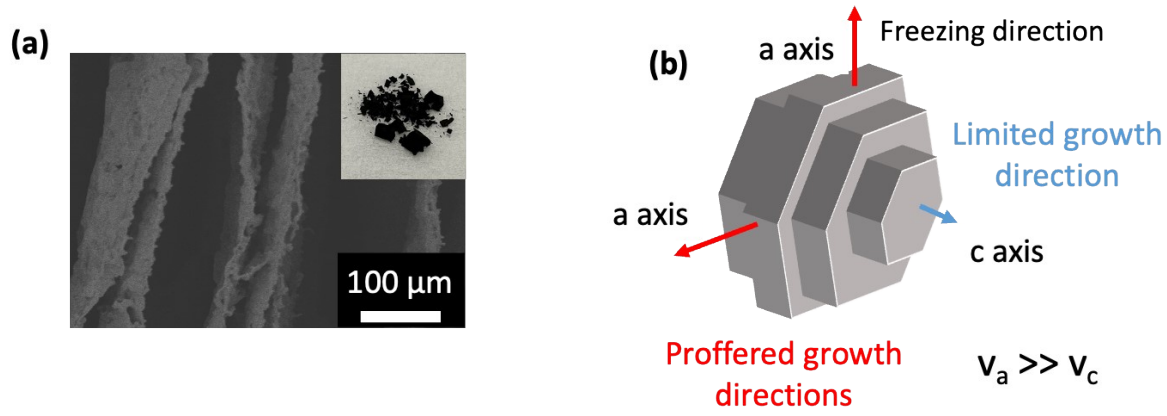

Figure S3. Ice-templated sample with a suspension containing only PR and CB. (a) SEM image of the corresponding sample. The inset image is an optical photo. (b) Illustration of ice growth in the absence of CNF.

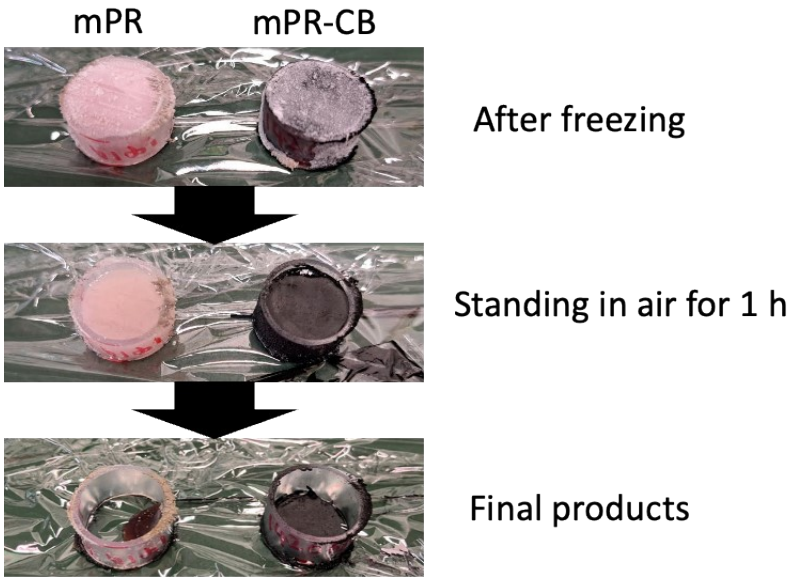

Figure S4. Optical images of unidirectionally frozen samples directly dried in air: mPR (left) and mPR-CB (right). While the samples retained their shapes after the ice melted when left in air for 1 h, they underwent significant shrinkage during subsequent ambient drying due to capillary forces.

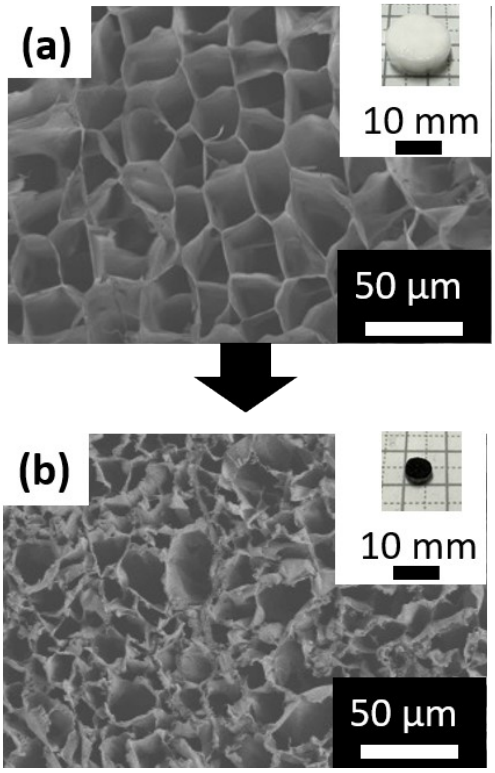

Figure S5. Morphology changes of mCNF by carbonization. (a) Axial cross-sectional SEM image of mCNF. (b) Axial direction SEM image of mCNF-9. Insets are optical images.

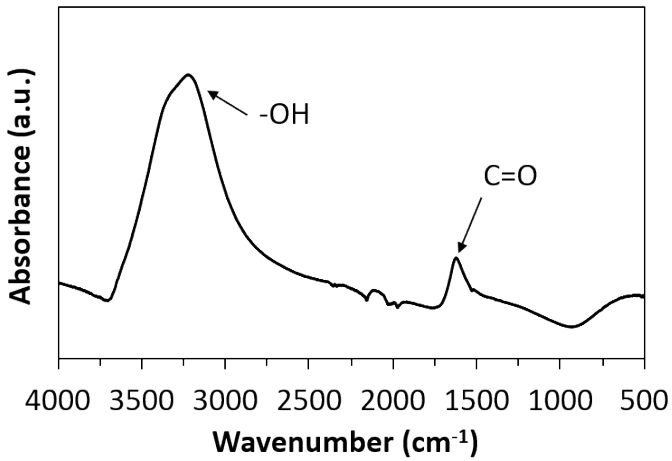

Figure S6. FT-IR spectrum of CB used in this work.

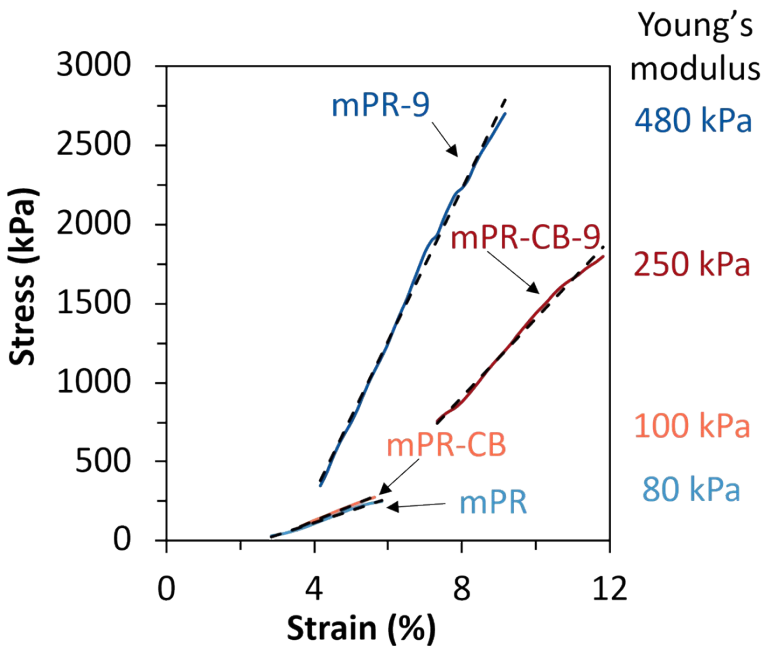

Figure S7. An enlarged view of the initial linear region in Figure 4a. Young's moduli were calculated by the slopes of the fitted dotted lines.

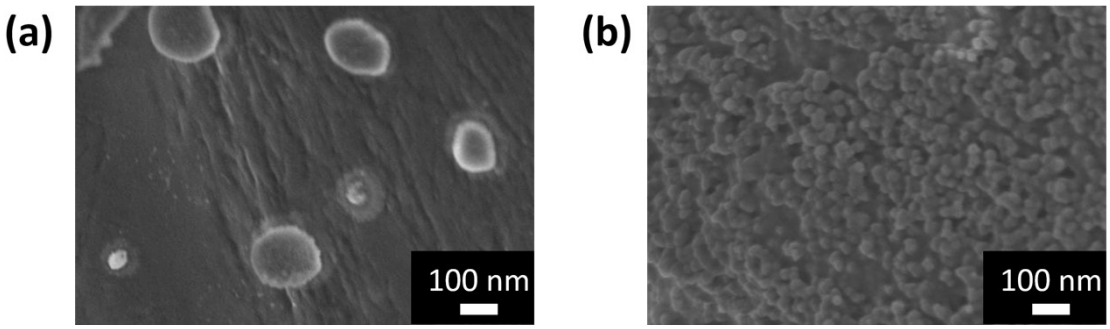

Figure S8. High-resolution SEM images. (a) mPR-9. (b) mPR-CB-9.

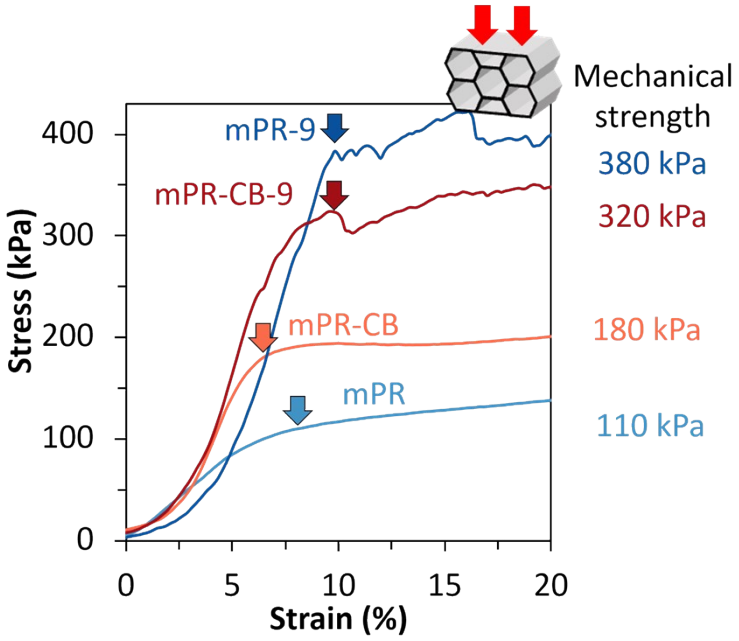

Figure S9. Radial compression stress-strain curves of mPR, mPR-9, mPR-CB, and mPR-CB-9. The arrows indicate the fracture points for each sample. The inset illustration indicates the compression direction.

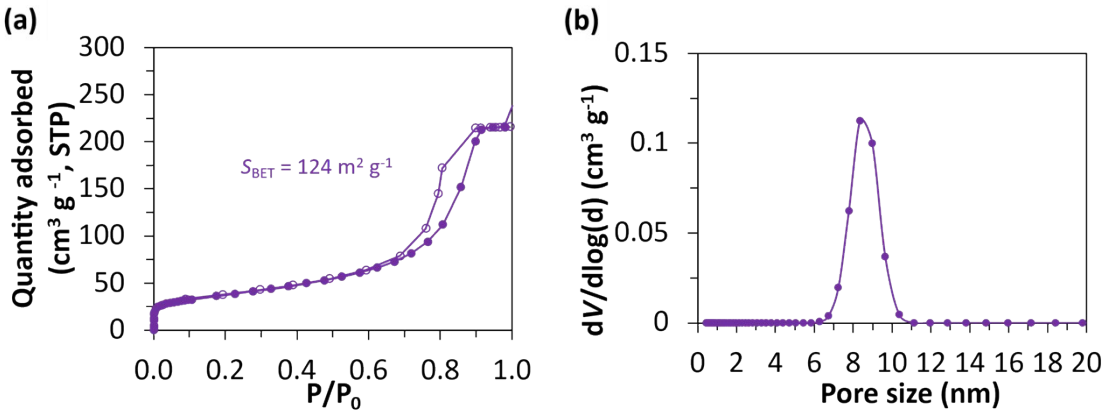

Figure S10. Porosity characteristics of CB. (a) N_2 adsorption-desorption isotherm. (b) Pore-size distribution.

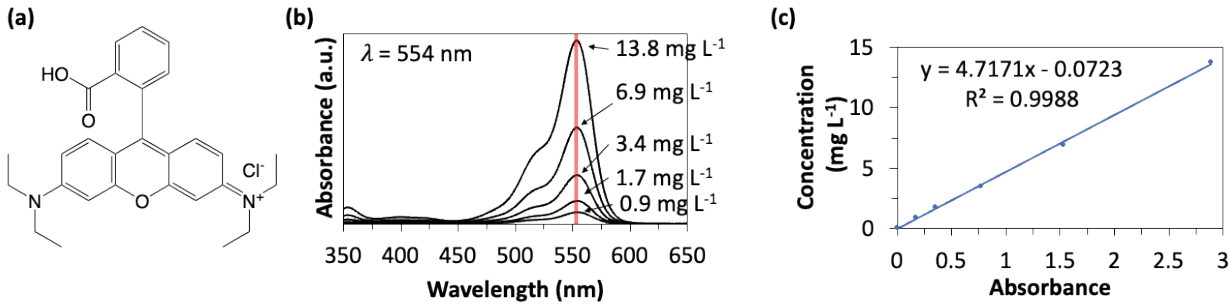

Figure S11. Calibration of RhB. (a) Molecular structure of RhB. (b) UV-Vis spectra of RhB solutions with various concentrations. (c) The calibration curve of RhB concentration.

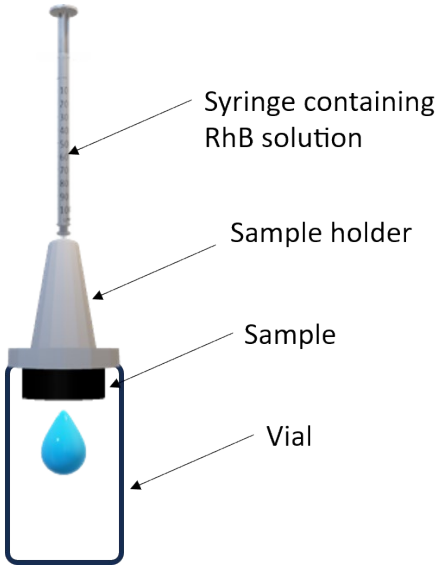

Figure S12. Illustration of the setup for RhB filtration.

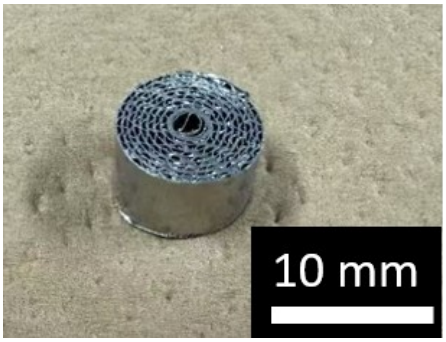

Figure S13. Optical image of the commercial metal-based honeycomb monolith.